Enhanced Limit Method for Slope Stability Analysis

Jaime Bojorque Iñeguez

Professor, Civil Engineering School, Faculty of Civil Engineering, Universidad de Cuenca, Ecuador
e-mail: jaime.bojorque@ucuenca.edu.ec

ABSTRACT

The aim of this paper is to investigate the Enhanced Limit Method, which combines finite element and limit equilibrium analysis in slope stability studies, and to describe its use in practical geotechnical applications. The study covers a critical review of the use of the finite element stress field inside a limit equilibrium analysis to assess slope stability. Particular emphasis is given to the common assumption of constancy of the factor of safety along the critical slip surface and the incorporation of the dilatancy angle, tensile strength, and Poisson's ratio. This study has shown that the factor of safety along the sliding surface is not the same, therefore, the assumption of constant safety factor of the Limit Equilibrium Method should be used with caution. It is found that the dilatancy and tensile strength have negligible effects on the determination of the factor of safety. They may, however, influence in some extend the location of the critical slip surface, particularly at the crest of the slope. The Poisson's ratio slightly affects the shear stresses without significant influence in the computation of the factor of safety. The representation of the local safety factors is better shown with the enhanced method, this feature is important because the location of the most critical zones can be assessed and used for guiding the implementation of remedial measures.

KEYWORDS: Slope Stability, Enhanced Limit Method, Finite Element, Limit Equilibrium, Factor of Safety.

INTRODUCTION

Slope stability is and remains a key research topic in geotechnical engineering because many engineering projects deal with natural and/or man-made slopes. In the literature, mainly three conceptual models are applied to slope stability analysis. First and the most used approach is the Limit Equilibrium Method (LEM), in which several formulations have been implemented that differ from each other basically in the number and the type of equilibrium equations used and in the considerations applied to the interslice forces (Pourkhosravani and Kalantari, 2011). Second, the Limit Analysis Method (LAM) where the lower- and upper-bound theorems are applied (Sloan, 1988; Sloan, 1989). Third and of increasing interest, are numerical techniques in which the most widely used are the Finite Element Method (FEM) (e.g. Lai et al., 2016) and the Finite Difference Method (FDM) (e.g. Mansour and Kalantari, 2011). These numerical methods fulfil the theoretical requirement for a complete solution, i.e., the complete set of equations of equilibrium, compatibility, constitutive laws and boundary conditions are applied.

To solve the problem of slope stability the system is represented by a mathematical model, this model can be simple or complex. If the mathematical model satisfies the four theoretical requirements, the solution is a full numerical method. Based on the numerical type, the method can be continuum (e.g., FEM, FDM), discontinuum (e.g., distinct elements) or hybrid (e.g., finite element-boundary element method). The FEM offers some benefits over existing methods for slope stability analysis. In this method, the geometry is discretized in small segments termed finite elements. Accuracy can be improved by using smaller elements and therefore more elements to represent a volume of soil. This results, however, in a trade-off between accuracy and calculation time.

The FEM, for slope stability analysis, has been mainly used in two approaches, a Direct Method and an Enhanced Limit Method (Naylor, 1982). In the direct method, the slope stability is determined by decreasing the shear strength (shear strength reduction technique) or by increasing the loads. The finite element strength reduction method (FE-SRM), has been increasingly used in research to analyze the slope stability in two- and three-dimensional problems (e.g. Xu et al., 2011). However, the acceptance of this method in the routine geotechnical practice for slope stability analysis still remains limited. This difficult incorporation in practical problems may be due to the long-term experience with limit equilibrium techniques. Another reason may due to that practicing engineers are often skeptical of the use of these methods for the increased need of soil data. This tendency will decrease when more and more staff with numerical model concepts is incorporated in geotechnical companies.

In the second approach, the Enhanced Limit Method (ELM), the results of a single finite element analysis, in this study, the state of stress produced by the body forces, are used for the search of the most critical surface by applying limit equilibrium concepts (Farias and Naylor, 1998; Fredlund et al., 1999; Krahn, 2003). This last category can be classified as Mixed (hybrid or coupled) methods, which combine concepts of different techniques.

The main idea behind mixed methods is to use the advantages of each technique for different aspects of the problem. Others combined approaches are the Rigid Finite Element Method (RFEM), in which FEM and LAM (Limit Analysis Method) concepts are used (Chen et al., 2003; Chen et al., 2004), FEM-LAM with linear and nonlinear programming (Kim, 2002), or Hybrid Finite-Discrete Element Method (An et al., 2016). It is worth noticing that these mixed techniques are increasingly using finite elements concepts to endure the applicability to complex problems. For example, the LAM has been incorporated into a numerical formulation that uses finite elements for the discretization of the soil mass. This type of formulation is referred as Finite Element Limit Analysis (Yu et al., 1998).

The present study pretend to explore the application of the combined finite element analysis and limit equilibrium analysis in slope stability studies and propose its use in practical geotechnical applications. The analysis covers a critical review of the use of the finite element stress field inside a limit equilibrium analysis to assess slope stability, considering linear elastic and nonlinear analysis. Particular emphasis is given to the common assumption of constancy of the factor of safety along the critical slip surface and the incorporation of the dilatancy angle, tensile strength, and Poisson's ratio.

MATERIALS AND METHODS

Enhanced Limit Method

For slope stability assessment the finite element stress results can be used in two distinct ways: the Strength Reduction Method (SRM) and the Enhanced Limit Method (ELM). The purpose of this section is to describe the use of ELM where the stress state determined from finite element analysis is combined with limit equilibrium concepts to assess the slope stability.

In ELM some assumptions used in limit equilibrium analysis are avoided, for example, the interslice force distribution, constant factor of safety, and normal force distribution conventions are not more involved. In conventional limit equilibrium analysis the factor of safety is constant along the entire slip surface. In reality, however, the local factor of safety is not constant, differing at each point. Therefore, in ELM the representation of the local safety is better which can guide the selection of critical zones. Moreover, it is known that the stresses computed from performing a limit equilibrium analysis do not represent the actual stresses within a soil mass. This difference is mainly due to the fact that LEM disregard the strain-stress relationship of the soil. In ELM, the slope stresses are closer to the actual stresses, compatibility criteria are fulfilled, and stage construction and excavation can be considered.

An advantage of ELM compared to finite element strength reduction is that for determining the factor of safety, only a single finite element analysis is needed, whereas in the SRM several finite element analyses have to be performed. However, it is important mentioning that different trials are necessary in order to determine the critical slip surface and assumptions of the failure mechanism are also used.

In finite element stress analysis soil parameter such as dilatancy angle, tensile strength, or Poisson's ratio are considered. Therefore, the influence of these parameters on the factor of safety and the critical slip surface computed with ELM are analyzed. Besides, the effect of the stress state by using a linear elastic or nonlinear material relationships is investigated.

Factor of Safety Definition in ELM

In the framework of ELM, three definitions for the factor of safety have been used (Fredlund and Scoular, 1999), including the strength (Kulhawy, 1969), stress (Zienkiewicz, 1975), and strength-stress level approach (Adikari and Cummins, 1985). The equations used to determine the factor of safety for each approach are presented in Figure 1. In these equations the terms used stand for: $\boldsymbol{FoS}$ is the factor of safety, $\boldsymbol{c}$ is the cohesion, $\boldsymbol{\phi}$ is the fiction angle, $\boldsymbol{\sigma_n}$ is the normal stress, $\boldsymbol{\tau}$ is the shear stress, $\boldsymbol{L}$ is the surface length, and the subscript $\boldsymbol{f}$ represents parameters at failure, $\boldsymbol{\sigma_1}$ and $\boldsymbol{\sigma_3}$ are the major and minor principal stresses, respectively. It can be seen that the strength-level approach computes the factor of safety as the ratio between the available shear strength of the soil and the actual shear stress, whereas, in the stress approach, the principal stress is increased until the failure envelop is reached.

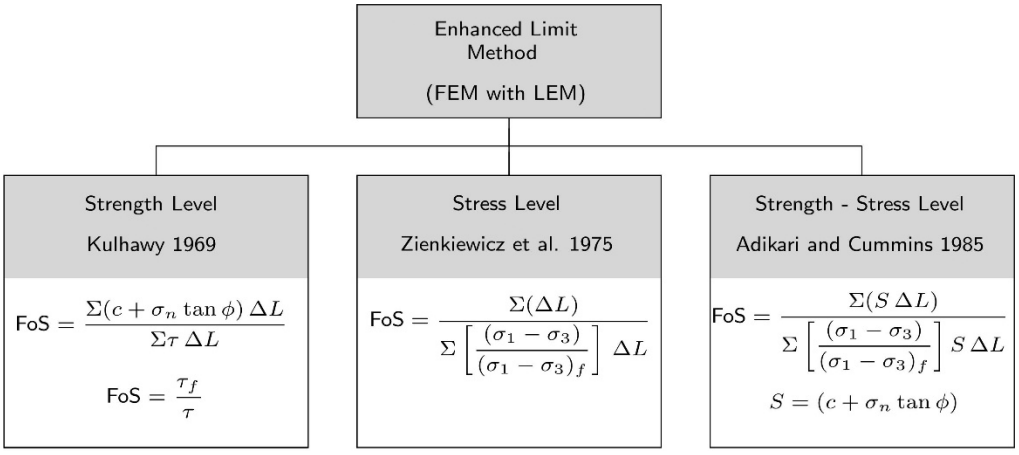

Figure 1: Different definition of factor of safety within the Enhanced Limit Method (after Fredlund and Scoular, 1999).

In this study, the strength-level approach is used because the orientation of the shear plane is taken into consideration and the concept is commonly used in slope stability analysis (Fredlund and Scoular, 1999). In this approach, the factor of safety of a slope is the ratio of the sum of available shear strength τ_f divided by the sum of shear stress τ along the length of a potential failure surface. Commonly, the integral is substituted with the summation of the slices along the trial surface, hence n is the number of slices and i represents the slice number.

$$FoS = \frac{\int \tau_{fi}\, dL}{\int \tau_{\imath}\, dL} = \frac{\sum_{i=1}^{n} \tau_{fi}\, \Delta L_i}{\sum_{\imath=1}^{n} \tau_{\imath}\, \Delta L_{\imath}} \tag{1}$$

The normal and shear stress acting along a trial slip surfaces are computed from the Cartesian stresses, from a finite element analysis, according to equation (2) and (3), respectively.

$$\sigma_n = \frac{\sigma_x + \sigma_y}{2} - \frac{\sigma_x - \sigma_y}{2}\cos(2\alpha_i) - \tau_{xy}\sin(2\alpha_i) \tag{2}$$

$$\sigma_n = \tau_{xy}\cos(2\alpha_i) - \frac{\sigma_x - \sigma_y}{2}\sin(2\alpha_i) \tag{3}$$

where σ_x, σ_y and τ_{xy} represent the horizontal, vertical and shear stress at point i, and α_i is the angle of a slice with respect to the horizontal, this angle is measured at the center of the slice.

The main idea behind the enhanced limit method is that a stress state determined from finite element analysis is used into a limit equilibrium analysis to assess the slope stability. The scheme of the enhanced limit process is shown in Figure 2. First, a finite element analysis, with linear elastic or elasto-plastic soil model, is performed. Then, the state of stress of the slope is exported into a limit equilibrium analysis.

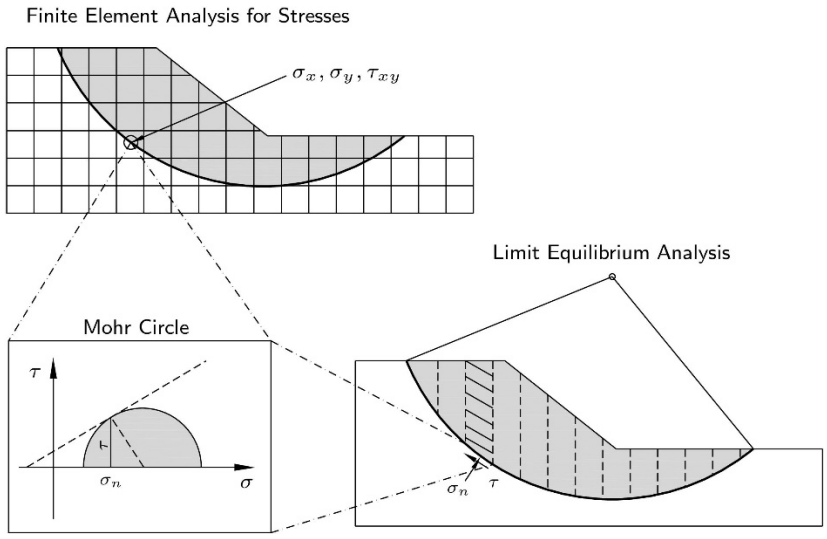

Figure 2: Schematic representation of the Enhanced Limit Method (adapted from Fredlund and Scoular, 1999).

Different techniques have been proposed to compute the stresses at a point in the trial slip surface, e.g., smoothing technique (Farias and Naylor, 1998). However, because high-order elements (15-node elements) are used in this finite element analysis (PLAXIS, 2007); a linear interpolation from the Gauss points is adequate to compute the stresses at any point. Once the stress field is determined, the normal and shear stress are computed for each slice center, then the local factor of safety is calculated as the ratio of the shear strength to the shear stress at the point. Then the global factor of safety is determined by equation (1). The slip surface which gives the lowest factor of safety is considered to be the critical slip surface and the factor of safety associated with it, is the factor of safety for the slope.

Search for the Critical Slip Surface

In a limit equilibrium context, there are several methods for the determination of the critical slip surface. These techniques can also be used in the enhanced limit method, where classical techniques such as Dynamic Programming Method (DPM) (Pham and Fredlund, 2003), Improved DPM (Zou et al., 1995), Broyden-Fletcher-Goldfard-Shanno (BFGS) (Kim and Lee, 1997), and the Complex Multi-Segment (Luo et al., 2012) to mention some, have shown promising results. Despite many advanced searching techniques have been proposed in the literature, for homogenous slopes the circular-shaped slip surface is adequate, and there is any reason to make the solution complex. In this study, a circular failure mechanism is used for the computation of the critical slip surface. This assumption is made because the studied slopes are composed of homogenous materials and numerical computation shows that, for homogeneous soil slope, slip bands are almost the same based on Bishop methods (Zhou et al., 2010). The search method is based on the grid radius method.

RESULTS AND DISCUSSION

Several finite element analyses using two homogeneous soil models with a slope inclination of 2H:1V and 1H:2V, are performed. These slope inclinations are in the typical range used in practical engineering. The height of the slope is 20 m with a unit weight γ = 20 kN/m^3, the soil

strength parameters are cohesion c = 40 kPa and friction angle ϕ = 30º. The assigned Young's modulus is 100 MPa. A fine mesh with 15-node triangular elements and standard boundary conditions are used in PLAXIS. The initial state of stresses is computed based on the gravity loading procedure. Ten different finite element analyses are discussed for the 2H:1V slope using 'original' soil strength parameters and five additional analyses using soil strength parameters reduced by a factor of 2 'reduced cases' (c_r = 20 kPa and ϕ_r = 16.1º from tanϕ/2) in order to investigate the behavior of the local safety factor near failure. Additionally, seven different analyses are performed for the 1H:2V slope, considering similar scenarios as for the 2H:1V case.

Simple Homogenous 2H:1V Slope

The geometrical configuration and finite element discretization used for the 2H:1V slope are shown in Figure 3. The boundaries are selected in order not to affect the location of the critical slip surface.

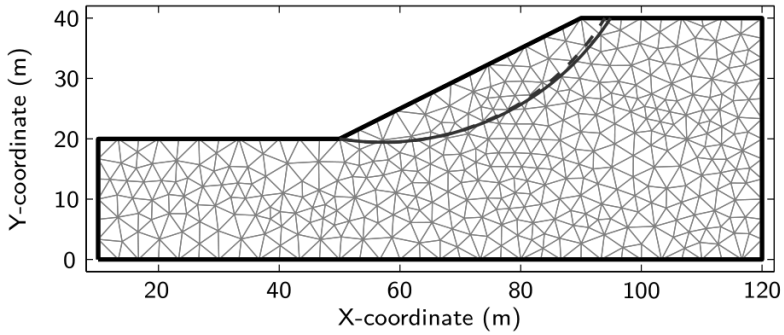

Figure 3: Geometrical configuration and discretization of the 2H:1V slope, and location of the critical slip surface, reference Case S1 (solid line) and Case S4 (dashed line).

Table 1 lists the cases and the corresponding factors of safety computed by FE-SRM (Finite Element Strength Reduction Method) and ELM (Enhanced Limit Method). Case S1 is taken as reference, which corresponds to an elasto-plastic analysis using the Mohr-Coulomb failure criterion. This case has a Poisson's ratio ν = 0.33, tensile strength equal to c/tanϕ, and dilatancy angle ψ = 0 (zero dilatancy non associated flow rule). Case S2 differs from S1 in the assigned Poisson's ratio (ν = 0.48). Two linear elastic analyses Case S3, with ν = 0.33 and Case S4, ν = 0.48, are performed to contrast with respect the elasto-plastic analyses.

Table 1: List of cases for the 2H:1V slope: for the original cases, c = 40 kPa and ϕ = 30º. For the reduced cases, soil strength parameters are reduced by a factor of 2, c_r = 20 kPa and ϕ_r = 16.1º

Case ID	Type of analysis	Poisson´s ratio	Tension	Dilatancy (ψ)	*FoS* FE-SRM	*FoS* ELM
S1	Plastic	0.33	c/tanϕ	0	2.331	2.347
S2	Plastic	0.48	c/tanϕ	0	2.327	2.362
S3	Elastic	0.33	-	-	-	2.337
S4	Elastic	0.48	-	-	-	2.410
S5	Plastic	0.33	c/tanϕ	ϕ(associated)	2.360	2.345
S6	Plastic	0.33	0	0	2.313	2.345
S7	Plastic	0.33	0	ϕ	2.341	2.345
S8Ex	Plastic	0.33	No	0	2.332	2.346

S9C5	P-5stages	0.33	c/tanϕ	0	2.310	2.349
S9C1	P-1stages	0.33	0	0	2.327	2.346
S1R	Plastic	0.33	c/tanϕ	0	1.169	1.172
S2R	Plastic	0.48	c/tanϕ	0	1.162	1.194
S3R	Elastic	0.33	-	-	-	1.168
S4R	Elastic	0.48	-	-	-	1.205
S5R	Plastic	0.33	c/tanϕ	ϕ	1.178	1.182
S6R	Plastic	0.33	0	0	1.155	1.174
S7R	Plastic	0.33	0	ϕ	1.175	2.345

Case S5 differs from Case S1 in the use of associated flow rule ($\psi = \phi$). Case S6 uses a tension-cut off equal to zero instead of c/tanϕ. In Case S7 both associated flow rule and tension-cut off equal to zero are used. To considerer the effect of excavation on the slope, three finite element analyses are performed in which different excavation cases are modelled, i.e., 5, 2 and 1 stage excavation. For all three excavation cases, the factors of safety determined by finite elements are equal to 2.332. As negligible differences are encountered for all excavation analysis, in the enhanced analysis only the excavation case with one stage (S8Ex) is presented. For Case 9, where the slope is built-up in different stages, the results are presented for five stages (S9C5) and one stage (S9C1) construction.

Since for the linear elastic cases, strength parameters are neglected, it is not possible to use the FE-SRM to compute the factor of safety. Thereby, only the values computed by ELM are given. It is worth noting that the factors of safety determined by FE-SRM and ELM are in very close agreement. For all cases the location of the critical slip surface is similar, corresponding to a toe sliding mechanism. The location of the critical slip surface for Case S1 is shown in Figure 3. It was observed that only for Case S4, elastic case with $\nu = 0.48$, a very slight difference appears at the crest of the surface. For this case the upper part of the slip surface is located 1 m apart from the other surface, without important effect (Figure 3).

Linear and Nonlinear Analysis

A comparative analysis is performed between the results of linear and nonlinear analysis. The shear strength and shear stresses computed along the critical circular surface for cases S1 to S4 are displayed in Figure 4.

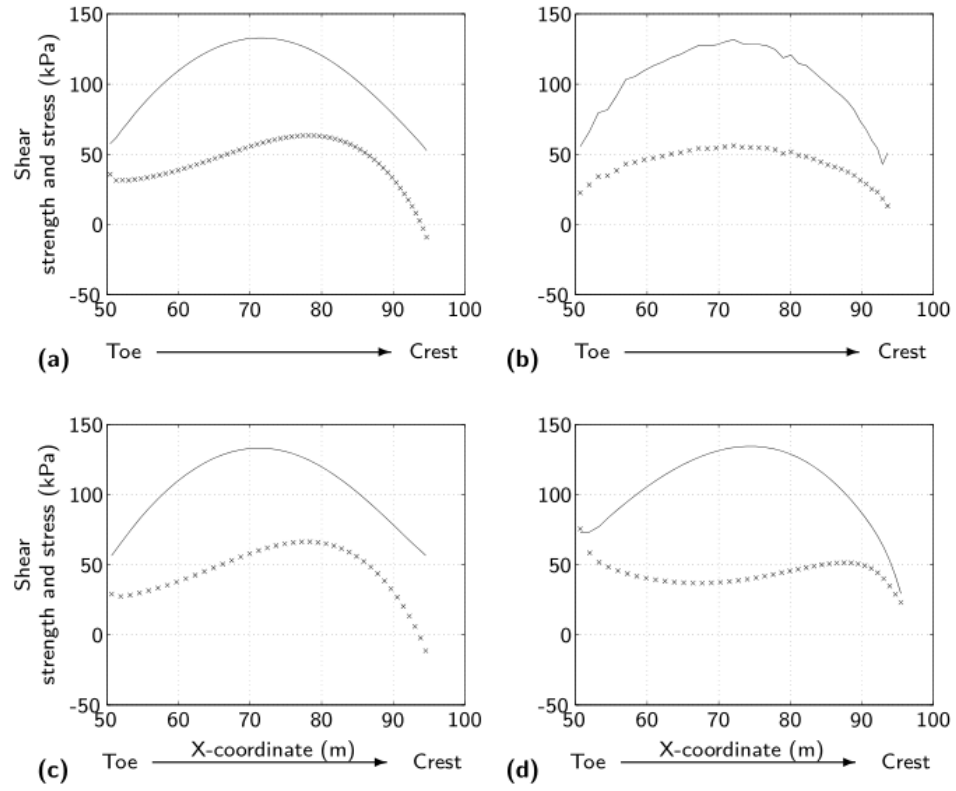

Figure 4: Shear strength (solid line) and shear stress (×) acting along the slip surface, 2H:1V slope: (a) S1, elasto-plastic $\nu = 0.33$; (b) S2, elasto-plastic $\nu = 0.48$; (c) S3, linear elastic $\nu = 0.33$; and (d) S4, linear elastic $\nu = 0.48$.

For the cases where $\nu = 0.33$ the shape and values of the shear forces are around the same (Figure 4a and 4c). At the crest of the slope, the stresses are zero or negative, indicating that forces are resisting the slide. However, for the cases where $\nu = 0.48$ the shear stress at the crest are always positive (Figure 4b and 4d). At the toe of the slope for the elastic case with $\nu = 0.48$ (Figure 4d), the shear stress is higher than the shear strength, thus the factor of safety in this zone is lower than one. However, this value has no physical meaning, this pattern is only due to the linear elastic model. In a nonlinear analysis the stresses are redistributed and this pattern is not present.

An advantage of the enhanced limit method is that local factors of safety can be evaluated. Figure 5 shows that the local factor of safety along the slip surface differs for all four cases. These figures describe better the distribution of stresses within the slope, which is an improvement with respect to the assumption of a constant factor of safety. For visualization purposes the local factor of safety, y-axis has been cut-off to a maximum value of 5. For the cases where $\nu = 0.33$ the shape and values of the local factor of safety are identical, showing an S-shaped curve (Figures 5a and 5c).

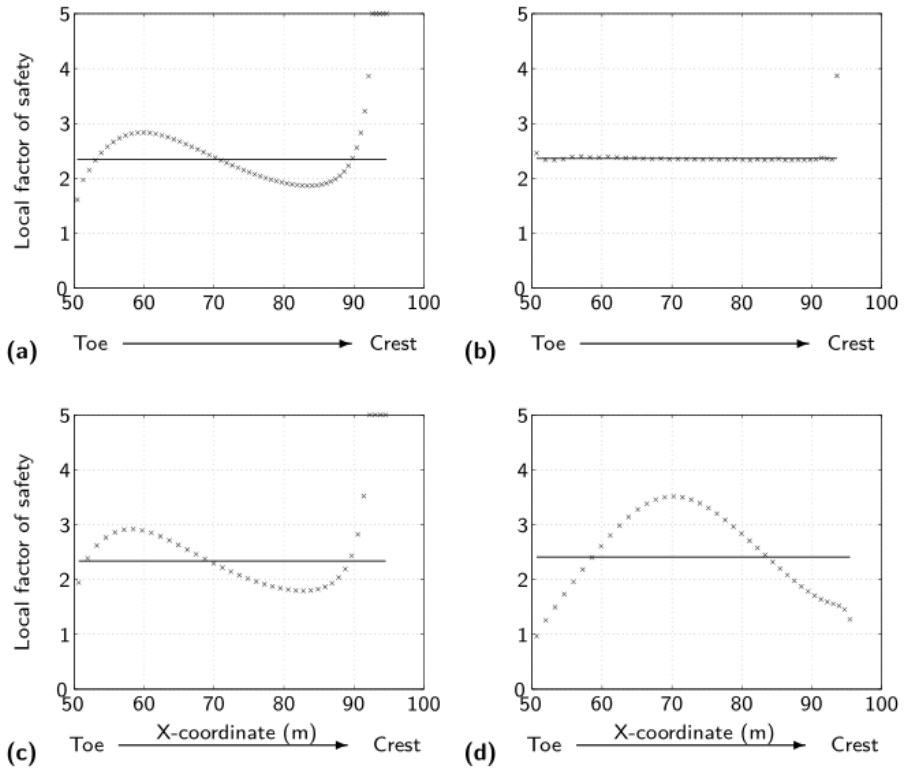

Figure 5: Local factor of safety (×), 2H:1V slope; global FoS (solid line): (a) S1, elasto-plastic v = 0.33, FoS=2.347; (b) S2, elasto-plastic v = 0.48, FoS=2.362; (c) S3, linear elastic v = 0.33, FoS=2.337; and (d) S4, linear elastic v = 0.48, FoS=2.410.

The toe of the slope is the critical zone representing a lower factor of safety, whereas the crest of the slope is resisting. Low factor of safety values are also presented at the middle of the slip surface. The variation of the local factor of safety for the elasto-plastic analysis with v = 0.48 is almost constant around the global factor of safety of 2.362 (Figure 5b). This pattern indicates that along the trial slip surface all the points have shear stresses that are a fraction of the shear strength (Figure 4b). Moreover, this linear pattern shows a rigid body motion of the slope. For the linear elastic analysis with v = 0.48 the local factor of safety has an inverted-U shape, presenting the lower factors at the toe and crest (Figure 5d).

The normal and shear stresses acting along the slip surface are presented as vectors in Figure 6. The distribution of normal and shear stress are almost identical for all the cases. However, there are small differences in magnitude for the normal forces at the toe and the crest in the elastic case with v = 0.48 (Figure 6b). As the location of the critical slip surface is nearly the same, the direction of the normal force remains.

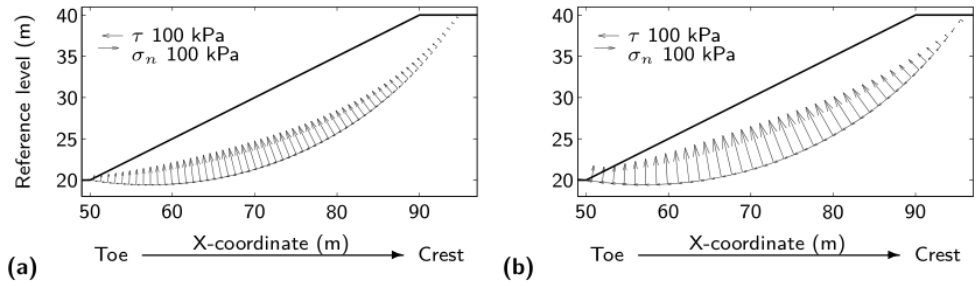

Figure 6: Distribution of normal and shear stress along the slip surface, 2H:1V slope: (a) S1, elasto-plastic $\nu = 0.33$ and (b) S4, linear elastic $\nu = 0.48$.

For the remaining elasto-plastic cases S5, S6 and S7 the results are similar to reference Case S1, indicating that, for this example, the dilatancy and the tensile parameter have small effect on the computation of both the factor of safety and the critical slip surface. For Case S8, no effect is produced in the stress state regarding the number of excavation stages. For Case S9 where the slope is built-up, some minor changes are found in the stress state; however, these differences have a negligible influence in the computation of both the factor of safety and the critical slip surface.

Reduced Strength Cases 2H:1V Slope

In this section, the reduced cases are considered where the strength parameters c and tanϕ are reduced by a factor of 2. It is not surprising that the location of the critical slip surface remains the same as that in the case without the reducing factor. This is because the same slip surface is expected when both strength parameters are multiplied by any scalar. The shear strength and shear stresses computed along the critical circular surface for cases S1R to S4R are shown in Figure 7.

The linear models, for some points, give shear stresses that are higher than the shear strength of the soil, which is physically not possible (Figures 7c and 7d). In the elasto-plastic models the shear stresses are always lower or equal to the shear strength (Figures 7a and 7b). Even though the linear models give shear stresses higher than the shear strength, the computed global factors of safety is relatively equal to the ones computed by elasto-plastic models.

The distribution of the local factor of safety for the elasto-plastic cases S1R and S2R compared to the liner elastic cases S3R and S4R are depicted in Figure 8. The local factors of safety for the elasto-plastic cases are always above unity; whereas, for the linear cases values lower that unity are computed. For example, Figure 8d shows that at the toe and the crest of the slope several local factors of safety are below one. For the other elasto-plastic cases S5R, S6R and S7R, the results are similar to reference Case S1R. As for the original strength values, this comparison indicates that the dilatancy and the tensile parameter, for this slope model, have negligible effect on the computation of both the factor of safety and the critical slip surface by ELM.

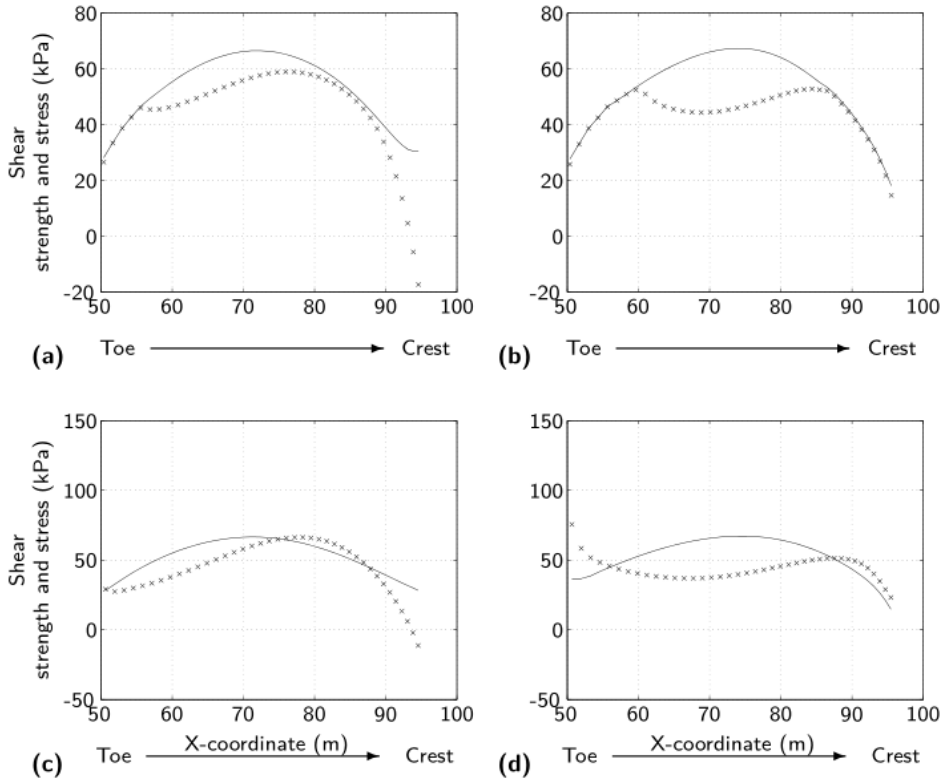

Figure 7: Shear strength (solid line) and shear stress (×) acting along the slip surface, 2H:1V slope: reduced cases (a) S1R, elasto-plastic $\nu = 0.33$; (b) S2R, elasto-plastic $\nu = 0.48$; (c) S3R, linear elastic $\nu = 0.33$; and (d) S4R, linear elastic $\nu = 0.48$.

Simple Homogenous 1H:2V Slope

In this example, seven different analyses are performed for a 1H:2V homogeneous soil slope with cohesion c = 40 kPa and friction angle $\phi = 30^{o}$. Table 2 lists the cases and corresponding factor of safety computed from FE-SRM and ELM. Similarly to the 2H:1V slope, Case T1 is taken as reference, which corresponds to an elasto-plastic analysis using the Mohr-Coulomb failure criterion, Poisson's ratio $\nu = 0.33$, tensile strength equal to c/tanϕ, and dilatancy angle $\psi = 0$. Case T2 differs from T1 in the assigned Poisson's ratio $\nu = 0.48$. Two linear elastic analyses Case T3 with $\nu = 0.33$ and Case T4, $\nu = 0.48$, are performed to contrast with the elasto-plastic analyses. Case T5 differs from Case T1 in the use of associated flow rule ($\psi = \phi$). Case T6 uses a tension-cut off equal to zero. Finally, in Case T7 both associated flow rule and tension-cut off equal to zero are used.

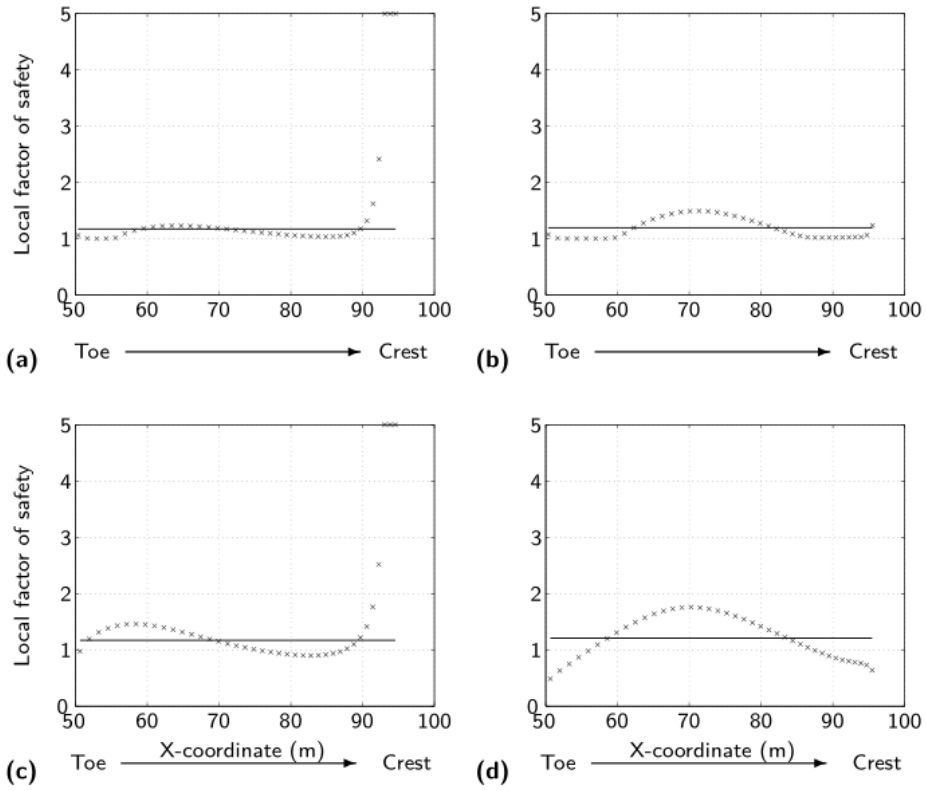

Figure 8: Local factor of safety (×), reduced 2H:1V slope; global FoS (solid line): (a) S1R, elasto-plastic ν = 0.33, FoS=1.172; (b) S2R, elasto-plastic ν = 0.48, FoS=1.194; (c) S3R, linear elastic ν = 0.33, FoS=1.168; and (d) S4R, linear elastic ν = 0.48, FoS=1.205.

Table 2: List of cases for a 1H:2V slope: c = 40 kPa and ϕ = 30°

Case ID	Type of analysis	Poisson´s ratio	Tension	Dilatancy (ψ)	*FoS* FE-SRM	*FoS* ELM
T1	Plastic	0.33	c/tanϕ	0	1.194	1.179
T2	Plastic	0.48	c/tanϕ	0	1.200	1.252
T3	Elastic	0.33	-	-	-	1.489
T4	Elastic	0.48	-	-	-	1.252
T5	Plastic	0.33	c/tanϕ	ϕ	1.278	1.182
T6	Plastic	0.33	0	0	1.151	1.180
T7	Plastic	0.33	0	ϕ	1.224	1.184

The search for the critical slip surface is performed with a circular shaped surface. For all cases the location where the critical slip surface developed is similar, corresponding to a toe sliding mechanism. The finite element model and location of the critical slip surface is shown in Figure 9.

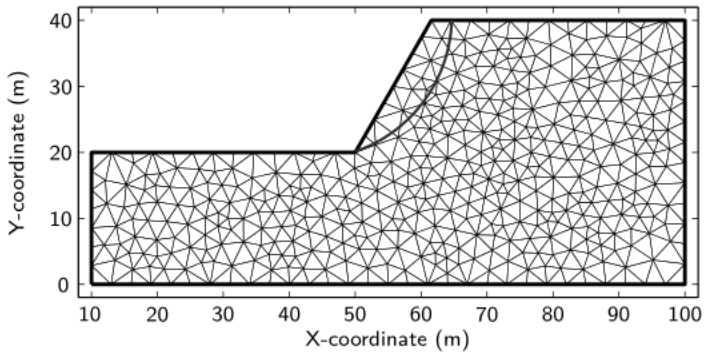

Figure 9: Finite element mesh and critical slip surface of the 1H:2V slope.

The shear strengths and shear stresses computed along the critical circular surface for cases T1 to T4 are displayed in Figure 10. At the crest of the slope the shear stresses are lower than the available shear strength. This distribution indicates that the crest of the slope is stable; however, it is worth to check tension crack development in this region. For the linear models (Figures 10c and 10d), as it was observed for the 2H:1V slope, there are zones where the shear stresses are higher that the resistance of the soil. This behavior is particularly important at the toe of the slope.

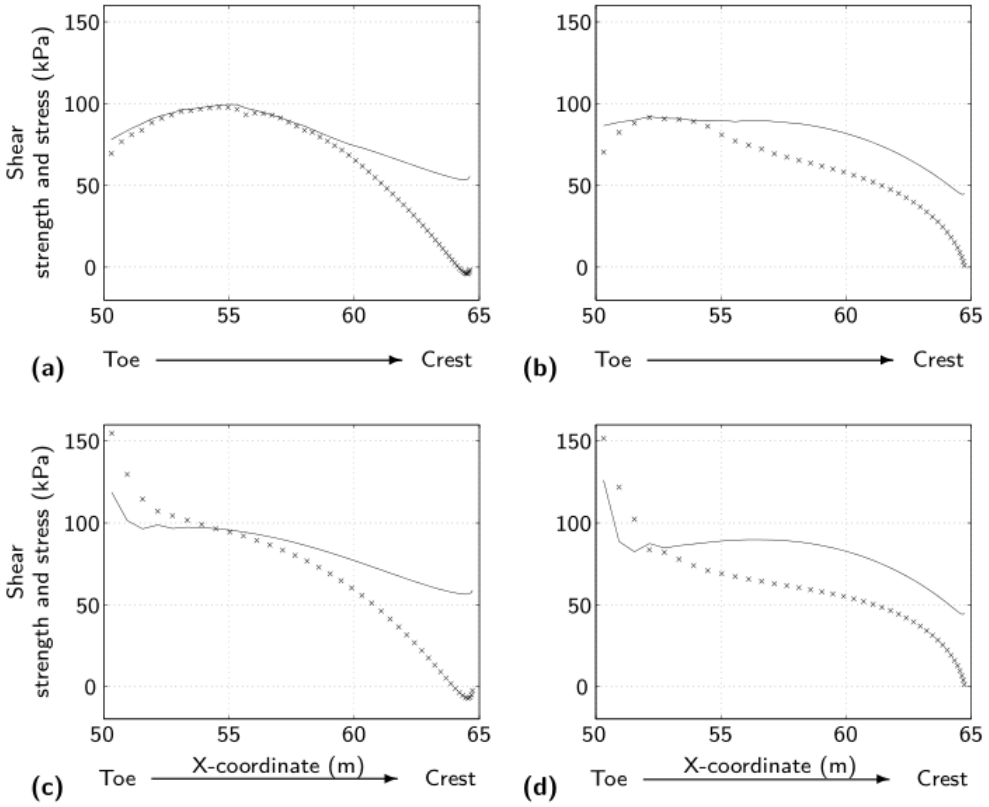

Figure 10: Shear strength (solid line) and shear stress (×) acting along the slip surface, 1H:2V slope: (a) T1, elasto-plastic $\nu = 0.33$; (b) T2, elasto-plastic $\nu = 0.48$; (c) T3, linear elastic $\nu = 0.33$; and (d) T4, linear elastic $\nu = 0.48$.

For the elasto-plastic models the shear stresses are lower or equal to the shear strength (Figures 10a and 10b). This pattern is a consequence of the redistribution of stresses in the nonlinear analysis. For the cases where the Poisson's ration is equal to 0.33, at the crest of the slope negative shear stresses are computed. For v = 0.48 the shear stresses are in the positive region.

The distribution of local factors of safety along the slip surface is shown in Figure 11. Case T1 (Figure 11a) shows that around two-thirds of the local factors of safety are below the global FoS of 1.179. For cases T2 and T4 (v = 0.48), around one-third is below the global FoS of 1.251 and 1.252, respectively (Figures 12b and 12d). The curve for Case T3 shows that half of the local factors of safety are below the global FoS of 1.149 (Figure 11c).

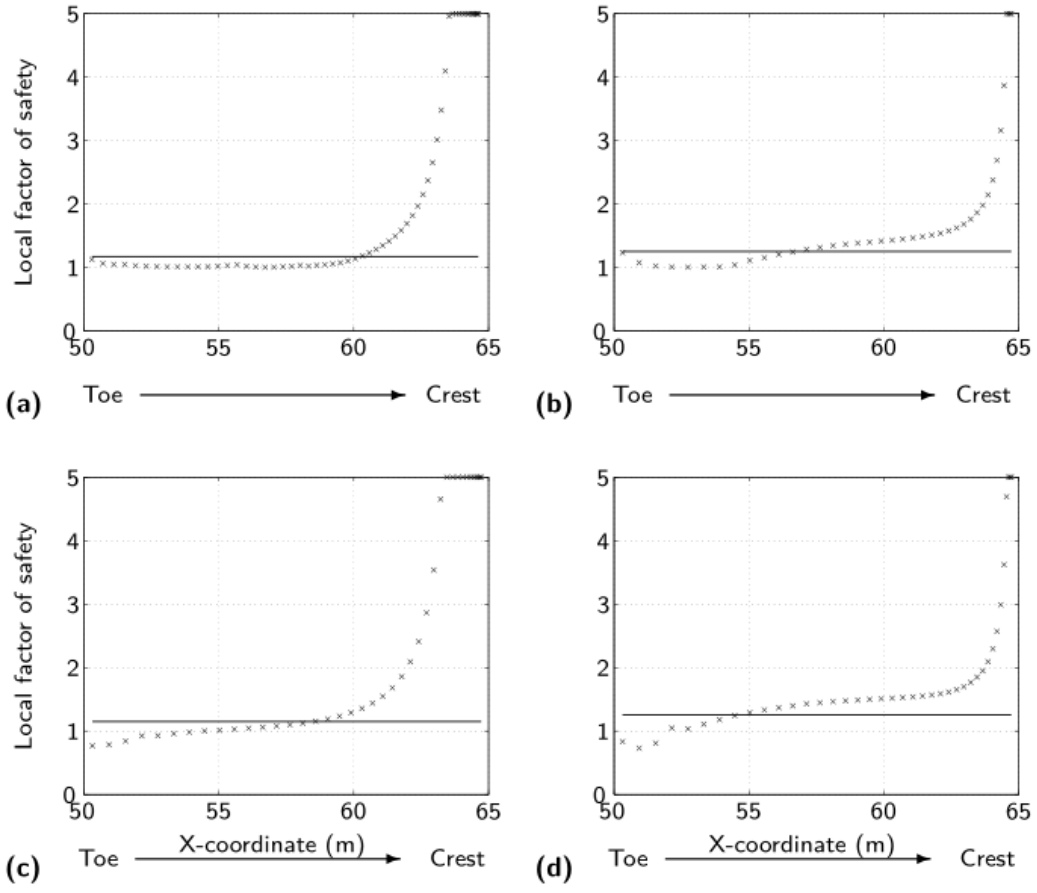

Figure 11: Local factor of safety (×), 1H:2V slope; global FoS (solid line): (a) T1, elasto-plastic v = 0.33, FoS=1.179; (b) T2, elasto-plastic v = 0.48, FoS=1.251; (c) T3, linear elastic v = 0.33, FoS=1.149; and (d) T4, linear elastic v = 0.48, FoS=1.252.

The location of the critical slip surface and value of the global factor of safety for cases T5, T6 and T7, are similar to reference Case T1. Additionally, the distributions of local factor of safety are similar to Case T1 (Figure 11a). Likewise the 2H:1V slope case, this comparison indicates that the dilatancy and the tensile parameter have negligible effects.

The normal and shear stresses acting along the slip surface is presented as vectors in Figure 12. The magnitudes of the stresses are indicated within the figure. The distribution of normal and shear stresses are similar for all the cases. However, there are small differences in magnitude for the normal forces at the toe in the elastic case with ν = 0.48 (Figure 12b).

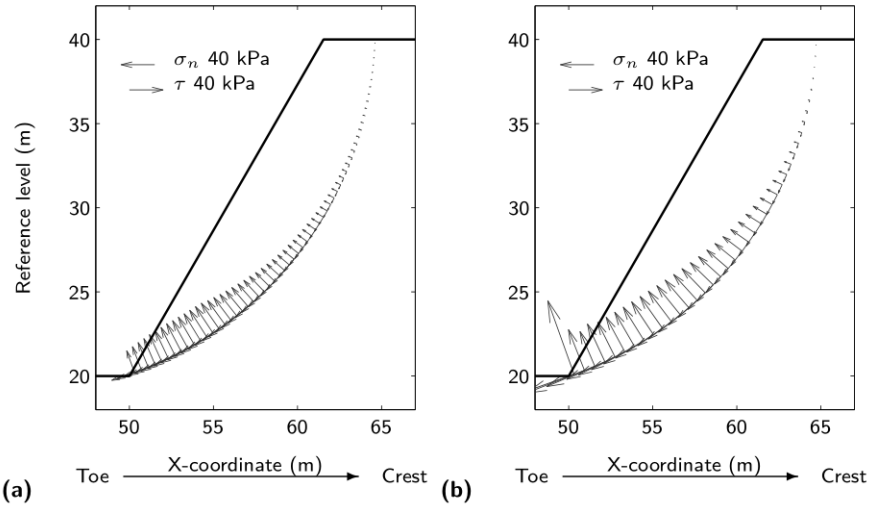

Figure 12: Distribution of normal and shear stress along the critical slip surface, 1H:2V slope: (a) T1, elasto-plastic ν = 0.33 and (b) T3, linear elastic ν = 0.33.

CONCLUSIONS

In this paper, the Enhanced Limit Method for slope stability is analyzed. In this method, the stress field derived from a finite element analysis is used to compute both the factor of safety and critical slip surface using limit equilibrium concepts. One advantage of ELM is that only one, linear or nonlinear, finite element computation is necessary, whereas, to determine the factor of safety by the strength reduction method, various nonlinear finite element analyses have to be executed. However, different limit equilibrium trials are necessary to determine a critical slip surface and assumptions of the failure mechanism are imposed.

Linear elastic analysis results are adequate to obtain an approximation of the stress distribution of a slope and to be used subsequently to compute the factor of safety and the critical slip surface. However, linear elastic analysis may compute stresses that are higher than the available soil strength, thus, giving for some points factors of safety below unity. By using a nonlinear analysis the points that are overstressed are redistributed allowing the neighbor elements to share the load.

The effect of dilatancy, tensile strength, and Poisson's ratio in ELM has been also assessed. It is found that the dilatancy and tensile strength have negligible effects on the determination of the factor of safety. They may, however, influence in some extend the location of the critical slip surface, particularly at the crest of the slope. The Poisson's ratio slightly affects the shear stresses without significant influence in the computation of the factor of safety.

Although the influence of water pressures and seismic forces are not included in this study, there is any limitation in applying this approach to such analyses. The ELM only needs the stress field computed in a finite element analysis. Therefore, in the ELM, the stresses computed during a dynamic earthquake or transient seepage analysis can be used to determine the factor of safety for each time that the stresses are available.

This analysis has also shown that the factor of safety along the sliding surface is not the same, therefore, the assumption of constant safety factor of the LEM should be used with caution. The representation of the local safety is better shown with ELM described in this paper. This feature is important because the location of the most critical zones can be assessed and used to guide the implementation of remedial measures.

REFERENCES

1. Adikari, G., and P.J., Cummins (1985) "An Effective Stress Slope Stability Analysis Method for Dams," 11th International Conference on Soil Mechanics and Foundation Engineering, Vol. 2, pp 713-722. San Francisco, USA.
2. An, Huaming, J. Shi, X. Zheng, and X. Wang (2016) "Hybrid Finite-Discrete Element Method Modeling of Rock Failure Processes in Brazilian Disc Tests," *Electronic Journal of Geotechnical Engineering*, Vol. 21, Bund. 07.
3. Chen, Jian, J. Yin, and C. Lee (2003) "Upper Bound Limit Analysis of Slope Stability Using Rigid Finite Elements and Nonlinear Programming," *Canadian Geotechnical Journal*, Vol. 40, No. 4, pp 742-752.
4. Chen, Jian, J. Yin, and C. Lee (2004) "Rigid Finite Element Method for Upper Bound Limit Analysis of Soil Slopes Subjected to Pore Water Pressure," Journal of Engineering Mechanics, Vol. 130, No. 8, pp 886-893.
5. Farias, M., and D. Naylor (1998) "Safety Analysis Using Finite Elements," Computers and Geotechnics, Vol. 22, No. 2, 165-181.
6. Fredlund, Delwyn G., R.E. Scoular, and N. Zakerzadeh (1999) "Using a Finite Element Stress Analysis to Compute the Factor of Safety," 52nd Canadian Geotechnical Conference, pp 73-80, Saskatchewan, Canada.
7. Fredlund, Delwyn G., and R.E. Scoular (1999) "Using Limit Equilibrium Concepts in Finite Element Slope Stability Analysis," International Symposium on Slope Stability Engineering, pp 31-47, Shikoku, Japan.
8. Kim, Jongmin, and S. Lee (1997) "An Improved Search Strategy for the Critical Slip Surface Using Finite Element Stress Fields," *Computers and Geotechnics*, Vol. 21, No. 4, pp 295-313.
9. Kim, Jongmin, R. Salgado, and J. Lee (2002) "Stability Analysis of Complex Soil Slopes Using Limit Analysis," *Journal of Geotechnical and Geoenvironmental Engineering*, Vol. 128, No. 7, pp 546-557.
10. Krahn, John (2003) "The 2001 R.M. Hardy Lecture: The Limits of Limit Equilibrium Analyses," *Canadian Geotechnical Journal*, Vol. 40, No. 3, pp 643-660.
11. Kulhawy, Fred Howard (1969) "Finite Element Analysis of the Behavior Of Embankments," Ph.D. thesis, University of California, Berkeley.

12. Lai, Jie, Y. Liu, X. Li, Y. Zheng, and Y. Wu (2016) "Dynamic Stability Analysis of Weathering Rock Slope by Strength Reduction Method," *Electronic Journal of Geotechnical Engineering*, Vol. 21, Bund. 08.

13. Luo, Suping, L. Zhao, D. Deng, and L. Li (2012) "Complex Multi-Segment Sliding Surface Search Method on Stability Analysis of Two-Dimensional Irregular Slope," *Electronic Journal of Geotechnical Engineering*, Vol. 17, Bund. G.

14. Mansour, Zeynadin S. and B. Kalantari (2011) "Traditional Methods vs. Finite Difference Method for Computing Safety Factors of Slope Stability," *Electronic Journal of Geotechnical Engineering*, Vol. 16, Bund. K.

15. Naylor, D. J. (1982) "Finite Elements and Slope Stability," Numerical Methods in Geomechanics, Vol. 92, pp 229-244. Reidel D. Publishing Company.

16. Pham, Ha T.V., and Delwyn, Fredlund (2003) "The Application of Dynamic Programming to Slope Stability Analysis," *Canadian Geotechnical Journal*, Vol. 40, No. 4, pp 830-847.

17. Plaxis (2007), 2D-Version 8, Finite Element Code for Soil and Rock Analyses. Delft, The Netherlands.

18. Pourkhosravani, Amin, and B. Kalantari (2011) "A Review of Current Methods for Slope Stability Evaluation," *Electronic Journal of Geotechnical Engineering*, Vol. 16, Bund. L.

19. Sloan, S.W. (1988) "Lower Bound Limit Analysis Using Finite Elements and Linear Programming," International Journal for Numerical and Analytical Methods in Geomechanics, Vol. 12, No. 1, pp 61-77.

20. Sloan, S.W. (1989) "Upper Bound Limit Analysis Using Finite Elements and Linear Programming," *International Journal for Numerical and Analytical Methods in Geomechanics*, Vol. 13, No. 3, pp 263-282.

21. Xu, Yingzi, J. Chatterjee, and F. Amini (2011) "A Comparative Slope Stability Analysis of New Orleans Levee Subjected to Hurricane Loading," *Electronic Journal of Geotechnical Engineering*, Vol. 16, Bund. C.

22. Yu, H.S., R. Salgado, S.W. Sloan, and J. Kim (1998) "Limit Analysis versus Limit Equilibrium for Slope Stability," *Journal of Geotechnical and Geoenvironmental Engineering*, Vol. 124, No. 1, pp 1-11.

23. Zhou, Yuan-wu, X. Tang, Z. Xiao, and E. Liu (2010) "Slope Slip Band Based on Circular Slip Surface," *Electronic Journal of Geotechnical Engineering*, Vol. 14, Bund. B.

24. Zienkiewicz, O.C., C. Humpheson, and R.W., Lewis (1975) "Associated and Nonassociated Visco-Plasticity in Soil Mechanics," Géotechnique, Vol. 25, No. 4, pp 671-689.

25. Zou, Jin-Zhang, D. Williams, and W. Xiong (1995) "Search for Critical Slip Surfaces Based on Finite-Element Method," *Canadian Geotechnical Journal*, Vol. 32, No. 2, pp 233-246.

Editor's note.
This paper may be referred to, in other articles, as:

Jaime Bojorque Iñeguez: "Enhanced Limit Method for Slope Stability Analysis" *Electronic Journal of Geotechnical Engineering*, 2016 (21.26), pp 10215-10232. Available at ejge.com.